High-frequency East Asia monsoon variability during 115000 - 93000 a BP in Northern China

Fengnian Wang[1], Yuejun Si[2,*], Baosheng Li[3,4], Dongfeng Niu[5], Xiaohao Wen[2], Zhiwen Li[6], Min Chen[2], Chen Wang[2], Yihua Guo[7], and Zhiying Yang[1]

[1] School of Geography and Tourism, Huizhou University, Huizhou, Guangdong, China
[2] School of Geography and Planning, Nanning Normal University, Nanning, Guangxi, China
[3] School of Geography, South China Normal University, Guangzhou, Guangdong, China
[4] State Key Laboratory of Loess and Quaternary Geology, Institute of Earth Environment, Chinese Academy of Sciences, Xi'an, Shanxi, China
[5] Lingnan Normal University, Zhanjiang, Guangdong, China
[6] College of Earth Science, East China Institute of Technology, Nanchang, Jiangxi, China
[7] Guangzhou Institute of Geography, Guangzhou, Guangdong, China

ABSTRACT

The FGS5c-d segment of the Fanjiagouwan section is located in the Salawusu River Valley on the southeast margin of the Mu Us Desert in China. It contains 17 sedimentary cycles consisting of aeolian dune sands and lacustrine facies during 115000 - 93000 a BP. Analyses of grain size and trace geochemical elements in the FGS5c-d segment revealed that the element contents were higher in lacustrine facies than in dune sands, displaying 17 element cycles that were similar to the sedimentary cycles in the FGS5c-d. The correlation between element contents and Mz(Φ)r was > 0.59. Grain size and trace geochemical elements during MIS5c-d indicate that 17 warm-humid and cold-arid climate cycles occurred in the FGS5c-d segment. This suggests that millennium-scale climate changes occurred in the alternations of the East Asian winter and summer monsoons during 115000 - 93000 a BP in the deserts of China and that these changes are the regional response to the global climate changes during that period.

1. INTRODUCTION

Desert is widely distributed in northern China and affected by the East Asian monsoons. Therefore, this area is important for studying the evolution of the paleo-environment and climate changes. Since the 1990s, Chinese and overseas scholars have discovered multiple cold and warm climate change periods in the MIS5 in ice cores (Dansgaard et al. 1993; Grootes et al. 1993; Taylor et al. 1993; Johnsen et al. 1995; Yao et al. 1997), oceans (Eglinton et al. 1992; Keigwin et al. 1994; McManus et al. 1994; Tu et al. 2001), loess (Ding et al. 1999; Fang et al. 1999; An 2000), desert (Li et al. 2000, 2005), and stalagmites (Cheng et al. 2019; Wu et al. 2020). This climate instability is important for understanding Quaternary global climate changes. It is still controversial as to whether or not more climate fluctuations occurred in the last interglacial MIS5, especially in the MIS5c or MIS5d (Field et al. 1994; Thouveny et al. 1994; An and Porter 1997; Li et al. 1998; Chen et al. 1999; Lu et al. 1999; Rousseau and Puisségur 1999; Guan et al. 2007). While MIS5 climate changes have been found in geological records around the world, the cold-warm climate change frequencies are different in each place. Therefore, more geological records of MIS5 changes will develop an understanding of global climate changes during that period. Since

* Corresponding author
  E-mail: 284561374@qq.com

2009, the Fanjiagouwan section (FGS) on the southeastern edge of the Mu Us Desert of China has continuously been investigated, and the FGS5c-d segment is found to contain 34 overlapping sedimentary sequences of dune sands and lacustrine facies. Its age is determined to be from 115000 to 93000 a BP, which is mainly aeolian sediment from the MIS5c-d period. Therefore, based on the sedimentary characteristics and ages of the FGS5c-d segment in the Fanjiagouwan section in the Mu Us Desert, the monsoonal climate variability indicated by the grain size and trace geochemical elements during the MIS5c-d period is discussed to supply new evidence for responding to the global climate changes in the desert of China during that period.

2. REGIONAL SETTING

The Fanjiagouwan stratigraphic section is located on the left bank in the middle reaches of the Salawusu River Valley, which is on the southeast margin of the Mu Us Desert, 37°43'57.3"N, 108°31'57.6"E. The annual average temperature of the Mu Us Desert is 6.0 - 8.5°C, and the annual precipitation is 250 - 440 mm, concentrated from July to September, accounting for 60 - 75% of the annually total precipitation, with large inter-annual precipitation variability. Since the late 1970s, researchers have found abundant geological information about monsoonal climate changes from the Salawusu River Valley in the Late Quaternary (Yuan 1978; Dong et al. 1983; Ding et al. 1996; Jin et al. 2007; Huang et al. 2009). Some researchers recently reported that the Milanggouwan section contains dune sands overlapping with fluvial or lacustrine facies in the Salawusu River Valley, with the age of the Late Quaternary, and the revealed sedimentary cycles correspond to the D/O cycles in the North Atlantic during the Late Quaternary (Li et al. 2000, 2005; Du et al. 2009, 2011; Si et al. 2014). The top of the section is 1293 m above sea level (Fig. 1). The total section thickness is nearly 80 m, and the outcropped thickness is about 63 m. The Fanjiagouwan section is mainly composed of aeolian paleo-mobile dune sands, depressions formed by flowing water, and lacustrine facies, all of which overlap each other (Fig. 2). The lithology and characteristics of sedimentary facies are nearly identical to the neighboring Milanggouwan section that has been previously studied (Li et al. 2000, 2005), mainly belonging to the Upper Pleistocene-Holocene periods. The Fanjiagouwan section is divided into 5 stages, FGS1 to FGS5 and their boundary ages are each equivalent to the time limits of the Greenland ice core or marine MIS1/MIS2/MIS3/MIS4/MIS5; FGS5 can be further divided into 5 sub-stages, FGS5a, FGS5b, FGS5c, FGS5d, and FGS5e, and their ages are each equivalent to MIS5a, MIS5b, MIS5c, MIS5d, and MIS5e.

The FGS5c-d segment is at a depth of 54.17 - 61.65 m of the Fanjiagouwan section, including sedimentary sequences 117LS - 150D.

3. MATERIALS AND METHODS

3.1 Ages

Ten OSL samples were collected from the FGS5c-d segment for OSL dating. The test materials were quartz particles ≤ 10 μm from the samples. OSL determination was completed by Zhao Hua in the OSL laboratory of the Institute of Hydrogeology and Engineering Geology of the Ministry of Geology and Mineral Resources of China. The test instruments are Type 1100 and 2200 OSL/TL produced by Daybreak in the United States.

3.2 Grain Size

Grain size samples were collected at an interval of 2 cm, and 374 samples were collected from the FGS5c-d segment of the Fanjiagouwan section. Pretreatment was conducted via the method proposed by Konert and Vandenberghe (1997): all samples were dried in an oven at a temperature < 40°C; an appropriate sample amount was taken into a 1000 ml beaker; hydrogen peroxide with a concentration of 30% and sufficient hydrochloric acid were added; then this was heated to boil for 20 min to remove organic matter and carbonate; next, 10 ml of dispersant $(NaPO_3)_6$ with a concentration of 0.5 mol L^{-1} were added to boil; after 24 hours, the solution was poured out and diluted; then the solution oscillated with an ultrasonic cleaner for 10 min; finally, the pretreated samples were analyzed for grain size. The instrument used was a Malvern Mastersizer 2000 M laser grain size analyzer with a measurement range of 0.02 - 2000 μm and an error of < 2%. Each sample was measured three times, and the average value was taken. All grain size data was stored in the database, and related parameters were calculated via Matlab. The grain size was expressed by its logarithmic Φ value, and the conversion formula is Φ = -log2d (with d being the diameter in mm) formulated by Krumbein and Aberdeen (1937). Grain size parameter calculations were conducted via the formula proposed by Folk and Ward (1957) Mz = (Φ16 + Φ50 + Φ84)/3; σ = (Φ84 - Φ16)/4 + (Φ95 - Φ5).

3.3 Trace Geochemical Elements

At intervals of 2 - 4 cm, 179 chemical element analysis samples were collected from the FGS5c-d segment of the Fanjiagouwan section. The test instrument was an X-ray fluorescence spectrometer (model: Epsilon 5) produced by Panac in the Netherlands. The samples and preparation processes were as follows: First, the sample was dried at a low temperature (< 40°C) and passed through a 2 mm sieve to remove debris, a vibration mill was used to grind the sample for 90 s, it passed through a 200 mesh (< 74 μm) sieve, then 6.0 g was taken from the sample with trimmed boric acid at the bottom, where it was held at 30 T for 30 s, and, finally, it was pressed into a 3.2 cm diameter round cake for testing.
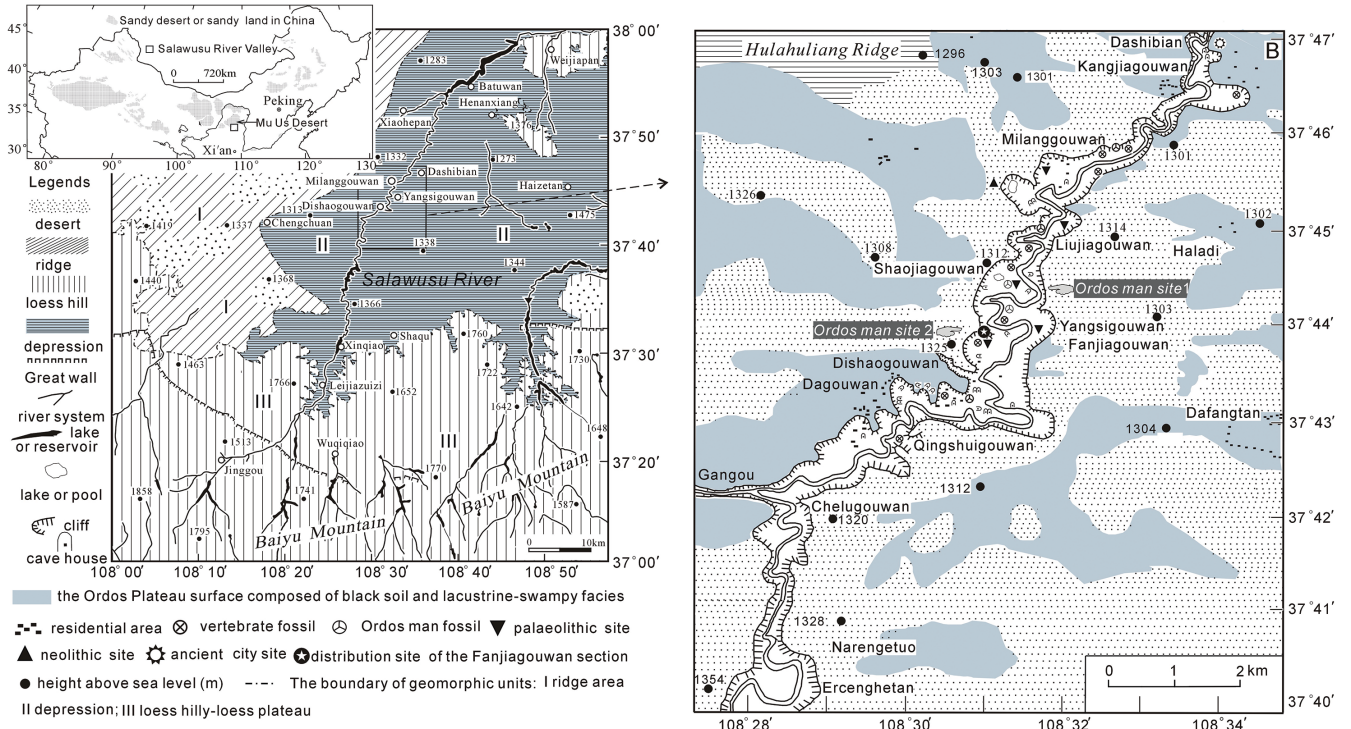
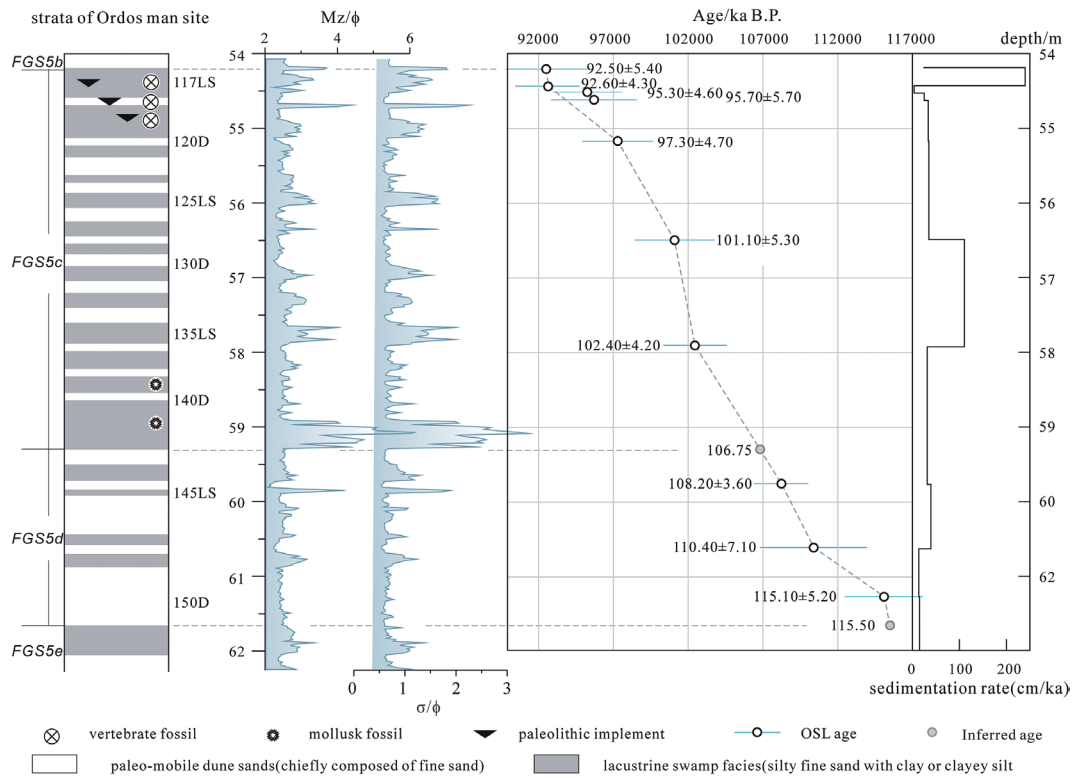Fig. 1. The location of the Salawusu River Valley and Fanjiagouwan section.

Fig. 2. Sedimentary sequences, ages, sedimentary rate and grain size parameter curves of the FWS5c-d segment in the Fanjiagouwan section.

Calibration was conducted with soil composition analysis standard materials (GSS2 - GSS28), 6 water-sediment analysis standard materials (GSD2a, GSD7a, GSD9 - GSD12), and 6 rock composition analysis standard materials (GSR1 - GSR6). In the experiment, GSS17 standard samples were added. The experimental error was ±5%, and the instrument detection limit was 1 μg g^{-1}.

4. RESULTS AND ANALYSIS

4.1 Ages

The dated ages and parameters of the FGS5c-d segment in the Fanjiagouwan section are listed in Table 1 and marked in Fig. 2. The age of the top of the FGS5c-d (at a depth of 54.17 m) was 92.50 ± 5.40 ka BP. While no dating result existed for its bottom (at a depth of 61.65 m), its age should be earlier than 115.10 ± 5.2 ka BP according to the age of 150D at a depth of 61.25 m. This was consistent with the age of MIS5c-MIS5d from 93 to 115 ka BP. Therefore, the FGS5c-d segment was considered to have formed during the MIS5c-MIS5d period. The boundary age of MIS5c/MIS5d is 104 ka, and in the FGS5c-d the age of 136D was 102400 ± 4200 a BP, and 144D was 108200 ± 3600 a BP. The geological boundary of MIS5c/MIS5d was taken at 141LS/142D in FGS5c-d. Based on dating results, the ages become older as the depth increases in the FGS5c-d segment, with ages/depths of 92.50 ka/54.17 m, 92.60 ka/54.37 m, 95.30 ka/54.57 m, 95.70 ka/54.62 m, 97.30 ka/55.16 m, 101.10 ka/56.48 m, 102.40 ka/57.92 m, 108.20 ka/59.77 m, 110.40 ka/60.63 m, and 115.10 ka/61.25 m.

4.2 Grain Size

Grain size analysis results showed that the FGS5c-d segment is mainly composed of the sand and that the sand content accounts for more than 90% in 3/4 samples. Among these, the fine sand content is highest, with the distribution range from 12.37 to 77.01%, and the average content of 61.90%; the content of very fine sand is higher, with the distribution range from 1.77 to 28.64%, and the average content of 15.66%; medium sand distribution range is from 2.82 to 35.03%, with an average content of 14.69%; coarse silt ranges from 0 to 32.89%, averaging 5.29%; fine silt ranges from 0 to 6.29%, averaging 0.72%; clay ranges from 0 to 30.04%, averaging 1.60%; coarse sand ranges from 0 to 3.81%, averaging 0.12%; and very coarse sand ranges from 0 to 1.42%, averaging 0.02%. To further illustrate sediment grain-size composition and sorting in the FGS5c-d segment, Fig. 2 charts the mean grain size (Mz) and standard deviation (σ), and Table 2 lists Mz(φ) and σ in different sedimentary facies. These show that Mz(φ) and σ display troughs in dune sands but peaks in lacustrine facies in the sedimentary cycles, and that 17 coarse-fine grain size cycles are formed in the FGS5c-d segment.

4.3 Trace Elements

In Table 3 and Fig. 3, it shows 11 trace element contents in modern mobile dune sands and paleo-mobile dune sands in Fanjiagouwan. Trace element distribution characteristics are as follows:

(1) The average contents of trace elements are similar in modern and paleo-mobile dune sands. Average contents of Mn, SR, and Zr range from 110.6 × 10^{-6} to 196.54 × 10^{-6}, with differences of 62.64 × 10^{-6}, 23.08 × 10^{-6}, and 19.05 × 10^{-6} in both dune sands, respectively; average contents of Zn, V, and Cr in both dune sands are also very similar, with differences of 16.4 × 10^{-6}, 6.41 × 10^{-6}, and 7.4 × 10^{-6}, respectively. The differences of average contents of Nb, Cu, and As are from 1.14 × 10^{-6} and 6.23 × 10^{-6}.

(2) Trace element contents are different from each other in the FGS5c-d segment. The average contents of P, S, Ti, Mn, Sr, Zr, and Ce are 342.67 × 10^{-6}, 2306.45 × 10^{-6}, 1798.10 × 10^{-6}, 258.41 × 10^{-6}, 311.96 × 10^{-6}, 141.84 × 10^{-6}, and 487.59 × 10^{-6}, each value is more than 140 × 10^{-6}, andthey range from 222 to 726 × 10^{-6}, 238 to 11497 × 10^{-6}, 1316 to 2780 × 10^{-6}, 154 to 955 × 10^{-6}, 133 to 1999 × 10^{-6}, 82 to 384 × 10^{-6}, and 433 to 529 × 10^{-6}, respectively. Average contents of Cr, V, Zn, As, and Nd are 50.26 × 10^{-6}, 41.30 × 10^{-6}, 19.35 × 10^{-6}, 10.99 × 10^{-6}, and 25.71 × 10^{-6}, each amount is from 100 to 10 × 10^{-6}, and they range from 23 to 77 × 10^{-6}, 26 to 61 × 10^{-6}, 11.9 to 35.4 × 10^{-6}, 0 to 38.3 × 10^{-6}, and 18 to 40 × 10^{-6}, respectively. Average contents of Cu, Ga, Nb, and La are 6.79 × 10^{-6}, 9.01 × 10^{-6}, 4.29 × 10^{-6}, and 2.79 × 10^{-6}, each of which is less than 10 × 10^{-6}, and they range from 2.6 to 13.9 × 10^{-6}, 5.8 to 11.2 × 10^{-6}, 2.9 to 7 × 10^{-6}, and 1.9 to 4.9 × 10^{-6}. Average content of Sn is 0.30 × 10^{-6}, and it ranges from 0.08 to 0.59 × 10^{-6}.

Figure 3 shows the changes in trace elements in the FGS5c-d segment. Among them, the average trace element contents in Mn, Sr, Zn, Cu, V, S, La, Nd, and P are relatively high in FGS5c and relatively low in FGS5d, but without obvious changes in the average contents of Nb, Ti, Ce, As, and Zr.

(3) The trace element distribution varied in different sedimentary facies. Different trace element contents were different in the same sedimentary facies, such as Mn, P, Nb, Zr, V, Cu, Ni, As, and Cr, but the same element had a similar content in the same sedimentary facies. This demonstrates a changing trend among the different sedimentary facies: the trace element contents increased from the dune sands to the overlying lacustrine facies. To better illustrate the relationship between grain size and trace elements, Fig. 4 plots scatter diagrams of Mz(φ) and each trace element content in the FGS5c-d segment. In the figure, as the Mz(φ) increased from dune sands to lacustrine facies, 11 trace element contents increased

Table 1. The OSL ages and parameters of the FGS5c-d segment.

Lab/horizon number	Depth/m	U (ppm)	Th (ppm)	K/%	Total dose (Gy)	Annual dose (GY)	ka BP
10G-528/117LS	54.17	1.70	4.60	1.28	210.07 ± 8.39	2.27	92.50 ± 5.40
10G-529/117LS	54.37	1.48	4.83	1.35	211.18 ± 4.19	2.28	92.60 ± 4.30
10G-530/117LS	54.57	1.13	3.73	1.51	217.35 ± 6.60	2.28	95.30 ± 4.60
10G-531/118D	54.62	1.21	5.40	1.46	231.51 ± 10.11	2.42	95.70 ± 5.70
10G-532/120D	55.16	1.20	4.24	1.63	239.06 ± 6.35	2.46	97.30 ± 4.70
10G-533/128D	56.48	0.76	3.34	1.42	200.40 ± 7.84	1.98	101.10 ± 5.30
10G-534/136D	57.92	1.66	4.40	1.56	262.15 ± 2.57	2.56	102.40 ± 4.20
10G-535/144D	59.77	1.43	3.68	1.56	256.53 ± 2.91	2.37	108.20 ± 3.60
10G-536/148D	60.63	0.79	3.05	1.43	223.65 ± 11.24	2.03	110.40 ± 7.10
10G-537/150D	61.25	0.97	3.33	1.42	242.78 ± 6.61	2.11	115.10 ± 5.20

Table 2. Mz(φ) and σ in different sedimentary facies in the FGS5c-d segment.

sedimentary facies (number of samples)		D (171)	LS (203)	FGS5c-d (374)
Mz (φ)	range	2.06 - 2.91φ	2.23 - 6.14φ	2.06 - 6.14φ
	average	2.46φ	2.89φ	2.69φ
σ	range	0.53 ~ 1.12	0.57 - 3.45	0.53 - 3.45
	average	0.65	1.09	0.89

Table 3. The trace geochemical element contents (×10⁻⁶) in different sedimentary facies in the FGS5c-d segment.

Sedimentary facies (Number)		Mn	P	Sr	Nb	Zr	V	Cu	As	Co	Cr	Zn
MD (8)	Min	125.80	74.50	120.00	4.50	67.60	22.80	3.10	1.80	3.60	21.40	16.00
	max	142.00	174.00	144.20	7.30	146.20	35.30	8.70	5.20	5.80	220.00	89.00
	ave	133.90	131.40	136.40	6.40	110.60	30.40	7.20	3.50	4.30	54.20	34.10
D (79)	Min	154.00	235.00	133.00	3.00	82.00	26.00	2.60	0	12.10	37.00	11.90
	max	335.00	554.00	263.00	7.00	384.00	54.00	9.30	32.70	27.20	69.00	23.60
	ave	196.54	322.15	159.48	4.12	129.65	36.81	6.06	9.73	18.98	46.80	17.70
LS (100)	Min	164.00	222.00	143.00	2.90	93.00	30.00	4.10	0	9.20	23.00	12.70
	max	955.00	726.00	1999.0	6.80	242.00	61.00	13.90	38.30	26.40	77.00	35.40
	ave	307.29	358.88	432.41	4.42	151.48	44.84	7.36	11.99	15.06	52.99	21.15

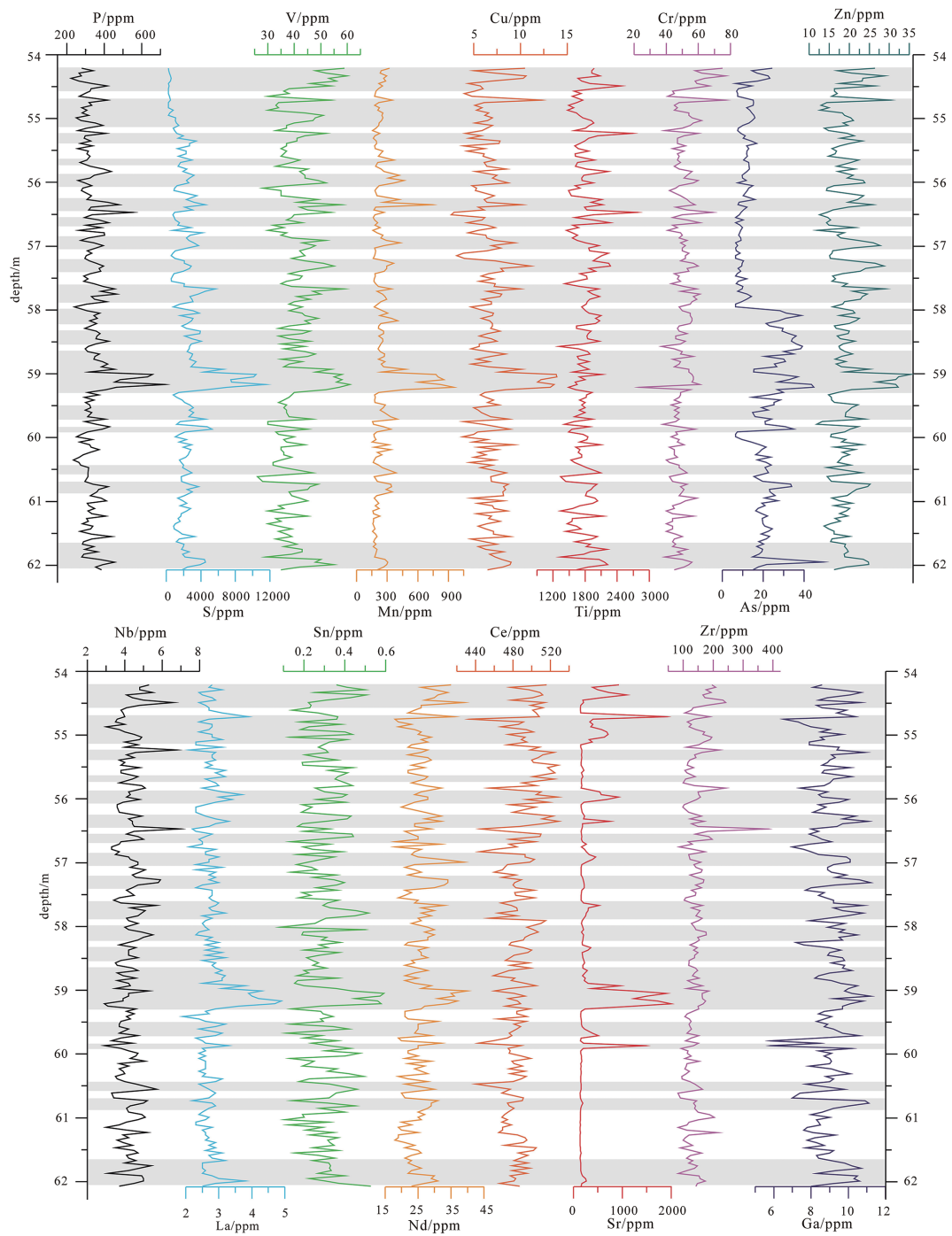Fig. 3. The distribution of trace elements in different sedimentary facies in the FGS5c-d segment.
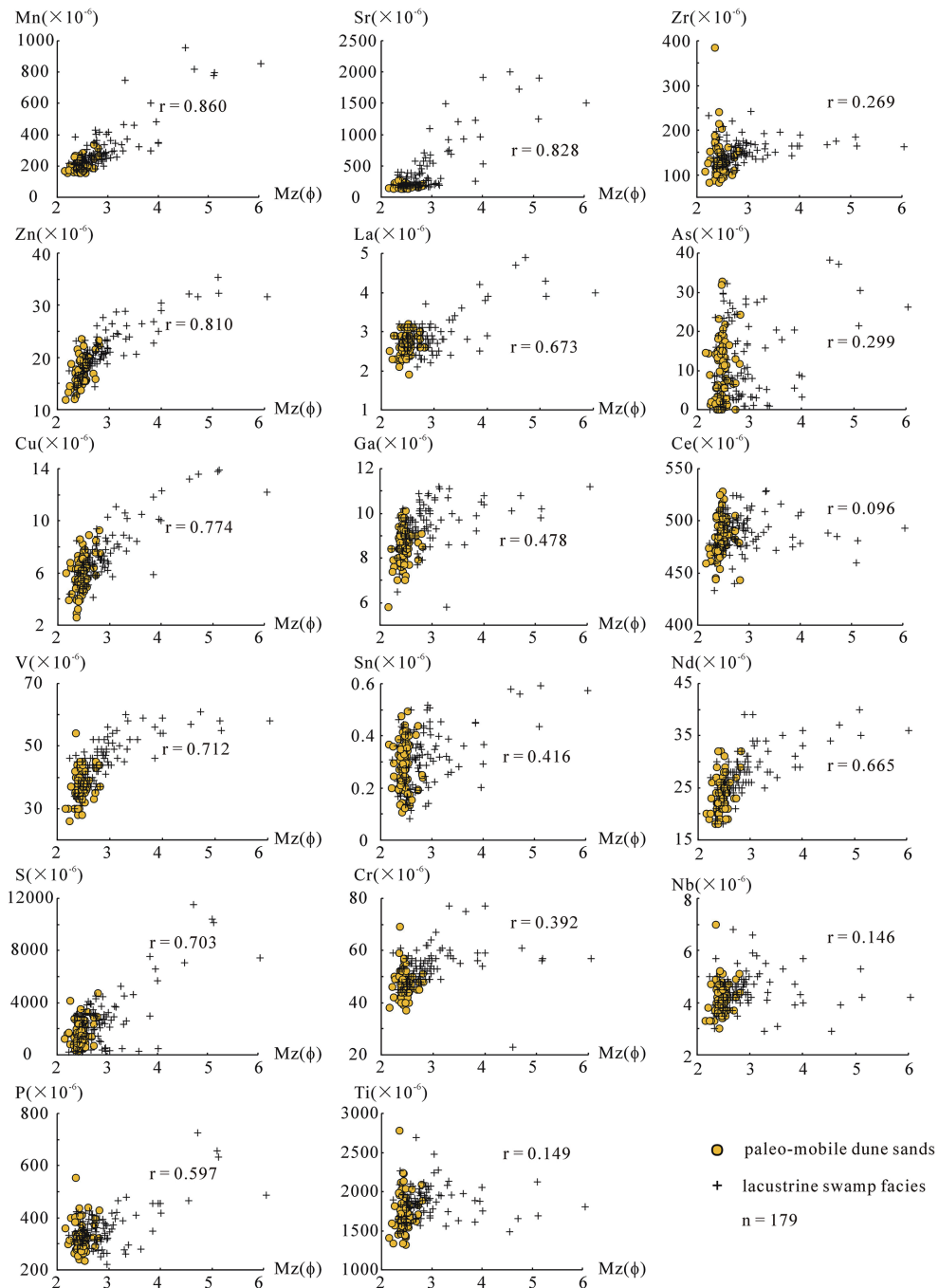
Fig. 4. Scatter diagram of Mz(φ) and trace geochemical element contents (×10⁻⁶) of the FGS5c-d segment.

accordingly, such as Mn and P, and their correlation is clear, with correlation coefficient r ranges from 0.41 to 0.86. In particular, 9 elements, Mn, Zn, Cu, V, S, P, Sr, La, and Nd are prominent, with their correlation coefficient r > 0.59.

Figure 4 shows the low values of Mn, P, Sr, Zn, V, Cu, and La correspond to the aeolian dune sands in the FGS5c-d segment; otherwise, their peaks correspond to the lacustrine facies. The contents of Ti, Zr, Ce, and Nb vary greatly in each sedimentary facies, but without any clear change to the tendency. The trace element contents display fluctuations in alternation between peaks and valleys in the FGS5c-d segment of the Fanjiagouwan section.

5. DISCUSSIONS

Table 3 shows that the distribution range and average values of most trace element contents in paleo-mobile dune sands were nearly the same as those in modern dune sands, it indicates that the sedimentary environment of paleo-mobile dune sands was similar to that of modern mobile dune sands. By comparison, Ou et al. (2006) reported that the grain size components and Mz(ϕ) were similar in both sands, but differences mainly existed between dune sands and lacustrine facies.

The field investigation revealed that the FGS5c-d segment was mainly composed of 34 sequences of dune sands and lacustrine facies that overlapped each other, with a stable stratigraphic structure and relatively developed horizontal beddings. Results showed that the geological ages were from old to new upward in the FGS5c-d segment, which followed the change discipline of stratigraphic sedimentation. Figure 2 shows a nearly linear relationship between age samples and depth, with the correlation coefficient r = 0.97. The sedimentary environment of the FGS5c-d is inferred to be relatively stable. Therefore, 34 sequences of dune sands overlapping with lacustrine facies in the FGS5c-d represent the alternating evolution in 17 cycles of aeolian sedimentation and lacustrine facies development in the Mu Us desert.

To probe the climate fluctuations in the FGS5c-d during the MIS5c-d period, it is necessary to understand the present climate and sedimentary processes in the study area. In the dry and cold winter and spring in the Mu Us Desert, the East Asian winter monsoon prevails, wind erosion increases and desertification is significantly enhanced; while in the warm and humid summer and autumn, the summer monsoon carries more precipitation, the water flow is strengthened, the lacustrine facies develop, and most dunes are fixed by the vegetation growing on them. Dune sands in the FGS5c-d t should have resulted from the paleo-East Asian winter monsoon that was similar to today winter monsoon. It is easy to understand the reason why the fossil egg debris of *Struthio* sp. was found in 118 D, which can survive in the arid desert environment. Otherwise, the fluvial-lacustrine facies indicate the precipitation carried by the paleo-East Asian summer monsoon during that period. For example, the snail fossils of *Vallonia patens* appeared in 139 LS and 141 LS, while its extant species currently lives in a warm and humid environment. This suggests that the FGS5c-d segment of the Fanjiagouwan section was affected by the strong East Asian winter and summer monsoons. In turn, 17 sedimentary cycles in the FGS5c-d segment composed of dune sands and lacustrine facies can be regarded as 17 cycles in alternations of the East Asian winter and summer monsoons.

Geochemical behaviors in the FGS5c-d segment also reflect the climate changes of 17 winter and summer monsoon cycles during the MIS5c-d period. When the dry and cold winter monsoon prevailed in the MIS5c-d period, Mz(ϕ) and σ of dune sands showed coarse-grained and well-sorted features (Fig. 2). Trace element contents resulted from the process of mechanical erosion, transportation, and accumulation. The element content differences in dune sands in different periods only reflect the differences between their source area and the "original rock" during the transportation process, and they underwent little chemical weathering after accumulation. During the strong East Asian summer monsoon periods, Mz(ϕ) and σ showed finer particles and poorly sorted characteristics (Fig. 2). Good hydrothermal conditions favor the biochemical weathering process. The highly active elements V, Cu, and Mn first leached from the surrounding positive terrain above the water surface and gathered with the water to the low-lying area where the section is located; if precipitation increases in a certain period, the water flow strengthens and stable elements that had previously remained on the positive terrain surface also converge in this area with flowing water, which accounts for why the trace element contents are higher in the lacustrine facies than in the underlying dune sands. In general, the stable elements P, Nb, and Zr, and the high-medium active elements V, Cu, and Mn can all gather in the lacustrine facies, which are related to the geomorphic position of the Fanjiagouwan section at that time. Most element contents are greatly affected by the sedimentary environment, the trace elements relatively migrate in the dune sands, and they relatively converge in the lacustrine facies.

The migration and aggregation of geochemical elements affected by topographical factors frequently occurred in the arid and semi-arid areas in northwestern China, such as Daihai, Inner Mongolia (Jin et al. 2006). The content changes of stable and active chemical elements in the lake sediments reflect that the leaching and migration of most elements are influenced not only by the summer monsoon and precipitation but also by the terrain.

In the context of overall warming during the last interglacial period, climatic fluctuations also exist, such as in the Mu Us Desert in China, with the paleo-aeolian dune sands developed among lacustrine facies in the FGS5c-d segment

serving as powerful evidence. This implies that when the dune sands accumulated, the winter monsoon was strong, the climate was relatively dry and cold, the migrated quartz and silicate minerals relatively increased, and the SiO_2 dilution effect of quartz (Li et al. 2005) caused the trace element contents to decrease. During the lacustrine facies development, the warm and humid climate favors soil and vegetation development. As a result, more clay particles and plant root adsorption can also increase the contents of some trace elements.

The FGS5c-d segment of the Fanjiagouwan section contains 34 overlapping dune sands and lacustrine facies sequences, displaying 17 grain-size and trace-element cycles, which represent 17 cycles of desert evolution and lacustrine facies development in the Mu Us Desert. This suggests that the Mu Us desert has experienced climate fluctuations in alternations of 17 winter and summer monsoons during the MIS5c-d period. The FGS5c-d segment lasts from 93 to 115 ka BP, and the average cycle duration is about 1300 a, which illustrates that the Mu Us desert has undergone a millennium-scale high-resolution desert evolution. Over the past years, the consistency of climate changes between East Asian monsoon cycles and Greenland ice core OIS5 during the last interglacial period has been continuously confirmed by many scholars (GRIP Members 1993; Li et al. 1998; North Greenland Ice Core Project Members 2004; Yuan et al. 2004; Cheng et al. 2009; Du et al. 2011, 2019; Galaasen et al. 2014; Pol et al. 2014; Helmens et al. 2015), and it is known that MIS5d represents the cold stage and MIS5c represents the warm stage (Christoph et al. 2002; Yuan et al. 2004; Dahl-Jensen et al. 2013; Cheng et al. 2019). Research results vary slightly in different areas because of different age models, study carriers, or indicator sensitivities. Overall, the FGS5c-d segment of the Fanjiagouwan section underwent similar climate changes to the MIS5c-d period as found in previous research: the FGS5d period was relatively cold, while the FGS5c period was relatively warm.

6. CONCLUSIONS

The grain size and trace geochemical elements of the FGS5c-d segment indicated that 17 warm-humid and 17 cold-dry climate changes occurred during 115000 - 93000 a BP in the Salawusu River Valley of the Mu Us Desert in China. This revealed millennium-scale East Asian monsoonal unstable climate changes, which were probably affected and controlled by the amounts of solar radiation and ice in the Northern Hemisphere. Lacustrine facies in the FGS5c-d segment resulted from a warm and humid environment, and dune sands resulted from a cold and dry environment. A sedimentary cycle consisting of dune sand and overlying lacustrine facies indicated a cold-dry and warm-wet climate cycle in the alternation of East Asian winter and summer monsoons. During the MIS5c-d period, the Mu Us desert experienced millennium-scale East Asian monsoonal climate fluctuations. Moreover, the Mu Us desert experienced 17 times the normal desertification process, 17 warm peaks in lacustrine facies, and 17 cold valleys in dune sands, which indicated the East Asian monsoonal climate instability in the MIS5c-d period.

REFERENCES

An, Z., 2000: The history and variability of the East Asian paleomonsoon climate. *Quat. Sci. Rev.*, **19**, 171-187, doi: 10.1016/s0277-3791(99)00060-8. [Link]

An, Z. and S. C. Porter, 1997: Millennial-scale climatic oscillations during the last interglaciation in central China. *Geology*, **25**, 603-606, doi: 10.1130/0091-7613(1997)025<0603:MSCODT>2.3.CO;2. [Link]

Chen, F. H., J. Bloemendal, Z. D. Feng, J. M. Wang, E. Parker, and Z. T. Guo, 1999: East Asian monsoon variations during Oxygen Isotope Stage 5: Evidence from the northwestern margin of the Chinese loess plateau. *Quat. Sci. Rev.*, **18**, 1127-1135, doi: 10.1016/S0277-3791(98)00047-X. [Link]

Cheng, H., R. L. Edwards, W. S. Broecker, G. H. Denton, X. Kong, Y. Wang, R. Zhang, and X. Wang, 2009: Ice Age Terminations. *Science*, **326**, 248-252, doi: 10.1126/science.1177840. [Link]

Cheng, H., H. Zhang, J. Zhao, H. Li, Y. Ning, and G. Kathayat, 2019: Chinese stalagmite paleoclimate researches: A review and perspective. *Sci. China Earth Sci.*, **62**, 1489-1513, doi: 10.1007/s11430-019-9478-3. [Link]

Christoph, S., A. Mangini, N. Frank, R. Eichstädter, and S. J. Burns, 2002: Start of the last interglacial period at 135 ka: Evidence from a high Alpine speleothem. *Geology*, **30**, 815-818, doi: 10.1130/0091-7613(2002)030<0815:SOTLIP>2.0.CO;2. [Link]

Dahl-Jensen, D., P. Gogineni, and J. White, 2013: Reconstruction of the last interglacial period from the NEEM ice core. *PAGES news*, **21**, 22-23, doi: 10.22498/pages.21.1.22. [Link]

Dansgaard, W., S. J. Johnsen, H. B. Clausen, D. Dahl-Jensen, N. S. Gundestrup, C. U. Hammer, C. S. Hvidberg, J. P. Steffensen, A. E. Sveinbjörnsdottir, J. Jouzel, and G. Bond, 1993: Evidence for general instability of past

climate from a 250-kyr ice-core record. *Nature*, **364**, 218-220, doi: 10.1038/364218a0. [Link]

Ding, Z. L., J. Z. Ren, and T. S. Liu, 1996: Millennial-scale monsoon-desert climate irregular variations and the mechanism during the Late Pleistocene. *Sci. China Ser. D-Earth Sci.*, **26**, 240-247.

Ding, Z. L., J. Z. Ren, S. L. Yang, and T. S. Liu, 1999: Climate instability during the penultimate glaciation: Evidence from two high-resolution loess records, China. *J. Geophys. Res.*, **104**, 20123-20132, doi: 10.1029/1999jb900183. [Link]

Dong, G., B. Li, and S. Gao, 1983: The case study of the vicissitude of Mu Us Sandy Land since the Late Pleistocene according to the Salawusu River strata. *Journal of Desert Research*, **3**, 9-14.

Du, S., B. Li, and D. Z. David, 2009: East Asian monsoons and the desert environment evolution recorded by $CaCO_3$ in MGS5 segment during the Last Interglacial in China's Salawusu River Valley. *Natural Science Process*, **19**, 1187-1193.

Du, S., B. Li, D. Niu, D. D. Zhang, X. Wen, D. Chen, Y. Yang, and F. Wang, 2011: Age of the MGS5 segment of the Milanggouwan stratigraphical section and evolution of the desert environment on a kiloyear scale during the Last Interglacial in China's Salawusu River Valley: Evidence from Rb and Sr contents and ratios. *Geochemistry*, **71**, 87-95, doi: 10.1016/j.chemer.2010.07.002. [Link]

Du, W., H. Cheng, Y. Xu, X. Yang, P. Zhang, L. Sha, H. Li, X. Zhu, M. Zhang, N. M. Stríkis, F. W. Cruz, R. L. Edwards, H. Zhang, and Y. Ning, 2019: Timing and structure of the weak Asian Monsoon event about 73,000 years ago. *Quat. Geochronol.*, **53**, 101003, doi: 10.1016/j.quageo.2019.05.002. [Link]

Eglinton, G., S. Bradshaw, A. Resell, M. Sarnthein, U. Pflaumann, and R. Tiedemann, 1992: Molecular record of secular sea surface temperature changes on 100-year timescales for glacial terminations I, II and IV. *Nature*, **356**, 423-426, doi: 10.1038/356423a0. [Link]

Fang, X., S. K. Banerjee, J. Li, X. Dai, and D. Guan, 1999: Environmental and rock magnetic studies of rapid fluctuations of Asian summer monsoon during the last interglacial maximum (MIS 5e). *Chin. Sci. Bull.*, **44**, 952-954, doi: 10.1007/bf02885074. [Link]

Field, M. H., B. Huntley, and H. Müller, 1994: Eemian climate fluctuations observed in a European pollen record. *Nature*, **371**, 779-783, doi: 10.1038/371779a0. [Link]

Folk, R. L. and W. C. Ward, 1957: Brazos River bar: A study in the significance of grain size parameters. *J. Sediment. Res.*, **27**, 3-26, doi: 10.1306/74d70646-2b21-11d7-8648000102c1865d. [Link]

Galaasen, E. V., U. S. Ninnemann, N. Irvalı, H. F. Kleiven, Y. Rosenthal, C. Kissel, and D. A. Hodell, 2014: Rapid reductions in north Atlantic deep water during the peak of the last interglacial period. *Science*, **343**, 1129-1132, doi: 10.1126/science.1248667. [Link]

GRIP Members (Greenland Ice-core Project Members), 1993: Climate instability during the last interglacial period recorded in the GRIP ice core. *Nature*, **364**, 203-207, doi: 10.1038/364203a0. [Link]

Grootes, P. M., M. Stuiver, J. W. C. White, S. Johnsen, and J. Jouzel, 1993: Comparison of oxygen isotope records from the GISP2 and GRIP Greenland ice cores. *Nature*, **366**, 552-554, doi: 10.1038/366552a0. [Link]

Guan, Q., B. Pan, H. Gao, B. Li, J. Wang, and H. Su, 2007: Instability characteristics of the East Asian Monsoon recorded by high-resolution loess sections from the last interglacial (MIS5). *Sci. China Ser. D-Earth Sci.*, **50**, 1067-1075, doi: 10.1007/s11430-007-0040-x. [Link]

Helmens, K. F., J. S. Salonen, A. Plikk, S. Engels, M. Väliranta, M. Kylander, J. Brendryen, and H. Renssen, 2015: Major cooling intersecting peak Eemian Interglacial warmth in northern Europe. *Quat. Sci. Rev.*, **122**, 293-299, doi: 10.1016/j.quascirev.2015.05.018. [Link]

Huang, Y. Z., N. A. Wang, and T. H. He, 2009: The desertification of the Mu Us Desert and its relationship with humans. *Chinese Geo-graphical Sciences*, **29**, 206-211.

Jin, H., M. Li, Z. Su, G. Dong, H. Zhao, and Z. Sun, 2007: Sedimentary age of strata in the Salawusu River Basin and climatic changing. *Acta Geologica Sinica*, **81**, 307-315.

Jin, Z., J. Cao, J. Wu, and S. Wang, 2006: A Rb/Sr record of catchment weathering response to Holocene climate change in Inner Mongolia. *Earth Surf. Process. Landf.*, **31**, 285-291, doi: 10.1002/esp.1243. [Link]

Johnsen, S. J., H. B. Clausen, W. Dansgaard, N. S. Gundestrup, C. U. Hammer, and H. Tauber, 1995: The Eem stable isotope record along the GRIP ice core and its interpretation. *Quat. Res.*, **43**, 117-124, doi: 10.1006/qres.1995.1013. [Link]

Keigwin, L. D., W. B. Curry, S. J. Lehman, and S. Johnsen, 1994: The role of the deep ocean in North Atlantic climate change between 70 and 130 kyr ago. *Nature*, **371**, 323-326, doi: 10.1038/371323a0. [Link]

Konert, M. and J. Vandenberghe, 1997: Comparison of laser grain size analysis with pipette and sieve analysis: A solution for the underestimation of the clay fraction. *Sedimentology*, **44**, 523-535, doi: 10.1046/j.1365-3091.1997.d01-38.x. [Link]

Krumbein, W. C. and E. J. Aberdeen, 1937: The Sediments of Barataria Bay. *J. Sediment. Res.*, **7**, 3-17, doi: 10.1306/d4268f8b-2b26-11d7-8648000102c1865d. [Link]

Li, B., D. D. Zhang, H. Jin, Z. Wu, M. Yan, W. Sun, Y. Zhu, and D. Sun, 2000: Paleo-monsoon activities of

Mu Us Desert, China since 150 ka B.P. — A study of the stratigraphic sequences of the Milanggouwan Section, Salawusu River area. *Palaeogeogr. Palaeoclimatol. Palaeoecol.*, **162**, 1-16, doi: 10.1016/s0031-0182(00)00101-2. [Link]

Li, B., D. D. Zhang, X. Wen, Y. Dong, Y. Zhu, and H. Jin, 2005: A multi-cycle climatic fluctuation record of the Last Interglacial Period: Typical stratigraphic section in the Salawusu River Valley on the Ordos Plateau, China. *Acta Geol. Sin.-Engl. Ed.*, **79**, 398-404, doi: 10.1111/j.1755-6724.2005.tb00905.x. [Link]

Li, L., Y. Sun, H. Lu, Z. Lai, and Z. An, 1998: Dust events of Chinese Loess Plateau during last interglacial and its comparison with the cold events of North Atlantic. *Chin. Sci. Bull.*, **43**, 90-93.

Lu, H., K. Van Huissteden, Z. An, G. Nugteren, and J. Vandenberghe, 1999: East Asia winter monsoon variations on a millennial time-scale before the last glacial-interglacial cycle. *J. Quat. Sci.*, **14**, 101-110, doi: 10.1002/(SICI)1099-1417(199903)14:2<101::AID-JQS433>3.0.CO;2-M. [Link]

McManus, J. F., G. C. Bond, W. S. Broecker, S. Johnsen, L. Labeyrie, and S. Higgins, 1994: High-resolution climate records from the North Atlantic during the last interglacial. *Nature*, **371**, 326-329, doi: 10.1038/371326a0. [Link]

North Greenland Ice Core Project Members, 2004: High-resolution record of Northern Hemisphere climate extending into the last interglacial period. *Nature*, **431**, 147-151, doi: 10.1038/nature02805. [Link]

Ou, X., B. Li, H. Jin, Z. Wu, X. Wen, G. Dong, L. Zeng, C. Ouyang, Y. Yang, and Y. Liu, 2006: Sedimentary characteristics of paleo-eolian dune sands in Salawusu Formation of the Salawusu River Valley. *Acta Geographica Sinica*, **61**, 965-975, doi: 10.11821/xb200609008. [Link]

Pol, K., V. Masson-Delmotte, O. Cattani, M. Debret, S. Falourd, J. Jouzel, A. Landais, B. Minster, M. Mudelsee, M. Schulz, and B. Stenni, 2014: Climate variability features of the last interglacial in the East Antarctic EPICA Dome C ice core. *Geophys. Res. Lett.*, **41**, 4004-4012, doi: 10.1002/2014gl059561. [Link]

Rousseau, D.-D. and J.-J. Puisségur, 1999: Climatic interpretation of terrestrial malacofaunas of the last interglacial in southeastern France. *Palaeogeogr. Palaeo-*

climatol. Palaeoecol., **151**, 321-336, doi: 10.1016/s0031-0182(99)00021-8. [Link]

Si, Y., B. Li, D. D. Zhang, X. Wen, F. Wang, S. Du, D. Niu, and Y. Guo, 2014: Climate fluctuation on a kiloyear scale during the Late Last Glacial in Mu Us Desert, China: Evidence from Rb and Sr contents and ratios. *Environ. Earth Sci.*, **72**, 4521-4530, doi: 10.1007/s12665-014-3352-0. [Link]

Taylor, K. C., C. U. Hammer, R. B. Alley, H. B. Clausen, D. Dahl-Jensen, A. J. Gow, N. S. Gundestrup, J. Kipfstuh, J. C. Moore, and E. D. Waddington, 1993: Electrical conductivity measurements from the GISP2 and GRIP Greenland ice cores. *Nature*, **366**, 549-552, doi: 10.1038/366549a0. [Link]

Thouveny, N., J.-L. de Beaulieu, E. Bonifay, K. M. Creer, J. Guiot, M. Icole, S. Johnsen, J. Jouzel, M. Reille, T. Williams, and D. Williamson, 1994: Climate variations in Europe over the past 140 kyr deduced from rock magnetism. *Nature*, **371**, 503-506, doi: 10.1038/371503a0. [Link]

Tu, X., F. Zheng, J. Wang, H. Cai, P. Wang, C. Bühring, and M. Sarnthein, 2001: An abrupt cooling event early in the last interglacial in the northern South China Sea. *Sci. China Ser. D-Earth Sci.*, **44**, 865-870, doi: 10.1007/bf02907077. [Link]

Wu, Y., T.-Y. Li, T.-L. Yu, C.-C. Shen, C.-J. Chen, J. Zhang, J.-Y. Li, T. Wang, R. Huang, and S.-Y. Xiao, 2020: Variation of the Asian summer monsoon since the last glacial-interglacial recorded in a stalagmite from southwest China. *Quat. Sci. Rev.*, **234**, 106261, doi: 10.1016/j.quascirev.2020.106261. [Link]

Yao, T., L. G. Thompson, Y. Shi, D. Qin, K. Jiao, Z. Yang, L. Tian, and E. M. Thompson, 1997: Climate variation since the Last Interglaciation recorded in the Guliya ice core. *Sci. China Ser. D-Earth Sci.*, **40**, 662-668, doi: 10.1007/bf02877697. [Link]

Yuan, B., 1978: Sedimentary environment and stratigraphical subdivision of Sjara Osso-Gol formation. *Chinese Journal of Geology*, **13**, 220-234.

Yuan, D., H. Cheng, R. L. Edwards, C. A. Dykoski, M. J. Kelly, M. Zhang, J. Qing, Y. Lin, Y. Wang, J. Wu, J. A. Dorale, Z. An, and Y. Cai, 2004: Timing, duration, and transitions of the Last Interglacial Asian Monsoon. *Science*, **304**, 575-578, doi: 10.1126/science.1091220. [Link]